

Article

# Direct Conversion of Methane to Methanol on Ni-Ceria Surfaces: Metal-Support Interactions and Water-enabled Catalytic Conversion by Site Blocking

Pablo G. Lustemberg, Robert M. Palomino, Ramon A Gutierrez, David C. Grinter, Mykhailo Vorokhta, Zongyuan Liu, Pedro J Ramirez, Vladimír Matolín, M. Veronica Ganduglia-Pirovano, Sanjaya D. Senanayake, and Jose A. Rodriguez

*J. Am. Chem. Soc.*, **Just Accepted Manuscript** • DOI: 10.1021/jacs.8b03809 • Publication Date (Web): 28 May 2018

Downloaded from <http://pubs.acs.org> on May 28, 2018

## Just Accepted

"Just Accepted" manuscripts have been peer-reviewed and accepted for publication. They are posted online prior to technical editing, formatting for publication and author proofing. The American Chemical Society provides "Just Accepted" as a service to the research community to expedite the dissemination of scientific material as soon as possible after acceptance. "Just Accepted" manuscripts appear in full in PDF format accompanied by an HTML abstract. "Just Accepted" manuscripts have been fully peer reviewed, but should not be considered the official version of record. They are citable by the Digital Object Identifier (DOI®). "Just Accepted" is an optional service offered to authors. Therefore, the "Just Accepted" Web site may not include all articles that will be published in the journal. After a manuscript is technically edited and formatted, it will be removed from the "Just Accepted" Web site and published as an ASAP article. Note that technical editing may introduce minor changes to the manuscript text and/or graphics which could affect content, and all legal disclaimers and ethical guidelines that apply to the journal pertain. ACS cannot be held responsible for errors or consequences arising from the use of information contained in these "Just Accepted" manuscripts.



ACS Publications

is published by the American Chemical Society, 1155 Sixteenth Street N.W., Washington, DC 20036

Published by American Chemical Society. Copyright © American Chemical Society. However, no copyright claim is made to original U.S. Government works, or works produced by employees of any Commonwealth realm Crown government in the course of their duties.

# Direct Conversion of Methane to Methanol on Ni-Ceria Surfaces: Metal-Support Interactions and Water-enabled Catalytic Conversion by Site Blocking

Pablo G. Lustemberg,<sup>[a]</sup> Robert M. Palomino,<sup>[b]</sup> Ramón A. Gutiérrez,<sup>[c]</sup> David C. Grinter,<sup>[d]</sup> Mykhailo Vorokhta,<sup>[e]</sup> Zongyuan Liu,<sup>[b]</sup> Pedro J. Ramírez,<sup>[c]</sup> Vladimír Matolín,<sup>[e]</sup> M. Verónica Ganduglia-Pirovano,<sup>\*,[f]</sup> Sanjaya D. Senanayake,<sup>\*,[b]</sup> and José A. Rodríguez<sup>\*,[b]</sup>

<sup>a</sup> Instituto de Física Rosario (IFIR), CONICET-UNR, Bv. 27 de Febrero 210bis, S2000EZF Rosario, Santa Fe, (Argentina)

<sup>b</sup> Chemistry Department, Brookhaven National Laboratory, Upton, NY 11973 (United States)

<sup>c</sup> Facultad de Ciencias, Universidad Central de Venezuela, Caracas 1020-A (Venezuela)

<sup>d</sup> Surfaces and Interfaces, Diamond Light Source, Harwell Science and Innovation Campus, Didcot Oxfordshire OX11 0DE (United Kingdom)

<sup>e</sup> Department of Surface and Plasma Science, Faculty of Mathematics and Physics, Charles University, Prague, (Czech Republic)

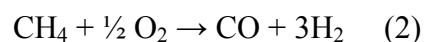
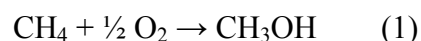
<sup>f</sup> Instituto de Catálisis y Petroleoquímica, CSIC, C/Marie Curie 2, 28049 Madrid (Spain)

\* Corresponding authors contact: [vqp@icp.csic.es](mailto:vqp@icp.csic.es) ; [ssenanay@bnl.gov](mailto:ssenanay@bnl.gov) ; [rodriguez@bnl.gov](mailto:rodriguez@bnl.gov)

**Abstract:** The transformation of methane into methanol or higher alcohols at moderate temperature and pressure conditions is of great environmental interest and remains a challenge despite many efforts. Extended surfaces of metallic nickel are inactive for a direct  $\text{CH}_4 \rightarrow \text{CH}_3\text{OH}$  conversion. This experimental and computational study provides clear evidence that low Ni loadings on a  $\text{CeO}_2(111)$  support can perform a direct catalytic cycle for the generation of methanol at low temperature using oxygen and water as reactants, with a higher selectivity than ever reported for ceria-based catalysts. On the basis of ambient pressure X-ray photoemission spectroscopy and density functional theory calculations, we demonstrate that water plays a crucial role in blocking catalyst sites where methyl species could fully decompose, an essential factor for diminishing the production of CO and  $\text{CO}_2$ , and in generating sites on which methoxy species and ultimately methanol can form. In addition to water-site blocking, one needs the effects of metal-support interactions to bind and activate methane and water. These findings should be considered when designing metal/oxide catalysts for converting methane to value-added chemicals and fuels.

## Introduction

Besides being an excellent source of energy, natural gas is a cheap and abundant source of carbon for the chemical industry. Methane is the primary component of natural gas and a potent greenhouse gas but it is difficult to convert it to upgraded fuels or chemicals due to the strength of the C–H bonds in the molecule (104 kcal/mol).<sup>1</sup> A synthetic path for a direct  $\text{CH}_4 \rightarrow \text{CH}_3\text{OH}$  transformation is a major goal in the industrial use of methane since the alcohol is useful as a fuel and a good building block for the generation of many chemical goods.<sup>1</sup> The reaction of molecular oxygen with methane can follow two different reaction paths:<sup>2</sup>



From a thermodynamic viewpoint, both reaction paths are exothermic, but at temperatures higher than 600 K, path (2) is more favourable.<sup>2</sup> Thus, to generate  $\text{CH}_3\text{OH}$  as a stable product or intermediate, one must find catalytic materials which can bind and activate  $\text{CH}_4$  at temperatures below 500 K.<sup>2-6</sup>

In recent years, the direct catalytic conversion of methane to methanol has sparked considerable interest.<sup>3-15</sup> The direct conversion is performed by the enzyme methane monooxygenase, but it is very difficult to use this biological system for major industrial-scale processes.<sup>7,10</sup> A core of three copper ions is probably responsible for the  $\text{CH}_4 \rightarrow \text{CH}_3\text{OH}$  transformation in the enzyme.<sup>4</sup> Copper-exchanged zeolites are able to mimic the activity of the methane monooxygenase.<sup>3-6,12</sup> Inside the structure of zeolites,  $\text{CH}_3\text{OH}$  can be generated by sequential dosing of  $\text{O}_2$  and  $\text{CH}_4$ , and at the end the alcohol is flushed out with  $\text{H}_2\text{O}$ .<sup>3-6</sup> A catalytic  $\text{CH}_4 \rightarrow \text{CH}_3\text{OH}$  conversion is also possible inside copper-exchanged zeolites<sup>12</sup> or on a model inverse oxide/metal catalyst such as  $\text{CeO}_2/\text{CuO}_x/\text{Cu}(111)$ .<sup>14</sup> In this study, we focus our

attention on the performance of a catalyst with a conventional Ni/CeO<sub>2</sub> configuration that can be used in technical applications. Using a combination of experiment (ambient pressure X-ray photoelectron spectroscopy) and theory (density functional calculations), we show that a low-loaded Ni/CeO<sub>2</sub>(111) system activates CH<sub>4</sub> at 300 K and then, with the help of water, which prevents sequential cleavage of C–H bonds, performs a direct catalytic cycle for the generation of CH<sub>3</sub>OH at relatively low temperatures (450 K). These results show the impact that metal-support interactions have on C–H and O–H bond breaking and the beneficial effect of water to diminish the production of CO and CO<sub>2</sub> during methane conversion to methanol. The mechanisms and outcomes demonstrated here are valid also for the production of other alcohols.

## Methods

**Experimental methods.** The experiments examining the conversion of methane into methanol over Ni/CeO<sub>2</sub>(111) surfaces were performed in an apparatus which contains an ultra-high vacuum (UHV) chamber for surface characterization and a batch micro-reactor for catalytic studies.<sup>16-18</sup> The UHV chamber was set up with X-ray photoelectron spectroscopy (XPS), Auger electron spectroscopy (AES), ion-scattering spectroscopy (ISS), low-energy electron diffraction (LEED), and temperature programmed desorption (TPD).<sup>16-18</sup> The Ni/CeO<sub>2</sub>(111) surfaces were prepared following the methodology described in detail in refs.<sup>16-18</sup> In the experiments of CH<sub>4</sub> activation, the sample was transferred *in vacuo* to the micro-reactor at room temperature then the hydrocarbon (1 Torr) was introduced. In the studies investigating the activity of the Ni/CeO<sub>2</sub>(111) catalysts for the conversion of methane to methanol, the samples were exposed to a mixture of 1 Torr of CH<sub>4</sub>, 0.5 Torr of O<sub>2</sub> and 0-4 Torr of H<sub>2</sub>O at room temperature and were rapidly heated to a reaction temperature of 450 K. Product yields (methanol, CO or CO<sub>2</sub>) were

determined by mass spectroscopy or gas chromatography. In these studies, data were collected in a systematic way at intervals of 5 min. The amount of molecules generated in the catalytic studies was normalized by the total reaction time and the active area exposed by the sample. The kinetic tests were always done in the limit of low conversion ( $< 10\%$ ).

The ambient-pressure XPS experiments for the Ni/CeO<sub>2</sub>(111) catalysts were performed at the Advanced Light Source in Berkeley, CA (beamline 9.3.2). The XPS spectra were recorded using a VG Scienta R4000 HiPP analyzer. A photon energy of 650 eV was used to excite the O 1s region. The C 1s, Ni 3p, and Ce 4d regions were probed with a photon energy of 490 eV. The total energy resolution in the photoemission experiments was  $\sim 0.2$  eV. For the binding energy calibration, we used the Ce 4d photoemission lines and their 122.8 eV satellite features.

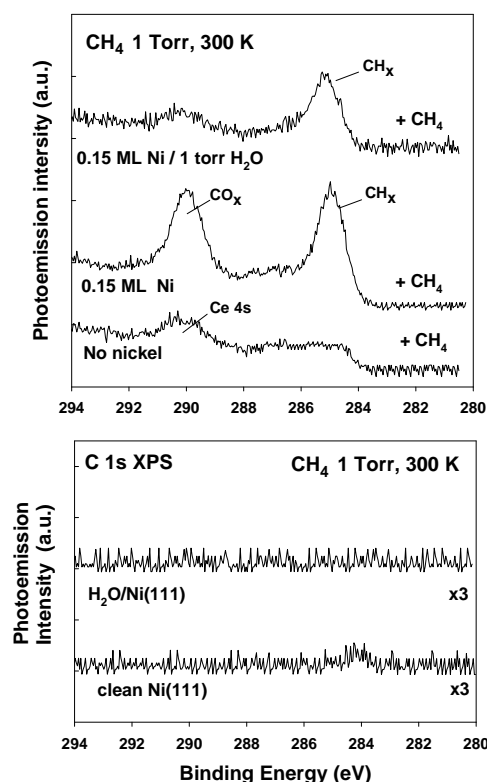
**Theoretical models and computational methods.** We performed spin-polarized density functional theory (DFT) calculations with the DFT+U procedure<sup>19</sup> (an effective onsite Coulomb interaction parameter,  $U$ , was applied to treat the Ce 4f states) and the Perdew, Burke, and Ernzerhof (PBE)<sup>20</sup> exchange-correlation functional (GGA). The Vienna ab initio simulation package (VASP)<sup>21</sup> was employed in this study. A value of 4.5 eV<sup>22,23</sup> was used for the Hubbard  $U$ -like term. The projector augmented wave method (PAW)<sup>24,25</sup> with a plane-wave cutoff of 415 eV was used. The C (2s, 2p), O (2s, 2p), Ni (3p, 3d, 4s), and Ce (4f, 5s, 5p, 5d, 6s) electrons were treated as valence states. The supported flat Ni<sub>4</sub> cluster on CeO<sub>2</sub>(111) surface was modeled by a (3×3) surface unit cell, with calculated ceria bulk equilibrium lattice constant (CeO<sub>2</sub>: 5.485 Å). The ceria surface was modeled employing a nine atomic layers (three O-Ce-O trilayers) slab geometry with at least 12 Å vacuum space. A Monkhorst-Pack grid with (3×3×1) was used. The atoms in the bottom trilayer were kept fixed at their optimized bulk-truncated positions during geometry optimization, whereas the others were allowed to relax. For the O<sub>2</sub>, H<sub>2</sub>O, CH<sub>4</sub> gas-

phase species,  $\Gamma$ -point calculations were performed using a  $(12 \times 12 \times 12)$  Å<sup>3</sup> box. The climbing image nudged elastic band method (CI-NEB)<sup>26</sup> was employed in order to locate the TS structures. For each reaction pathway, NEBs contained nine images. only one imaginary frequency was found for each of the TS structures reported in this work.

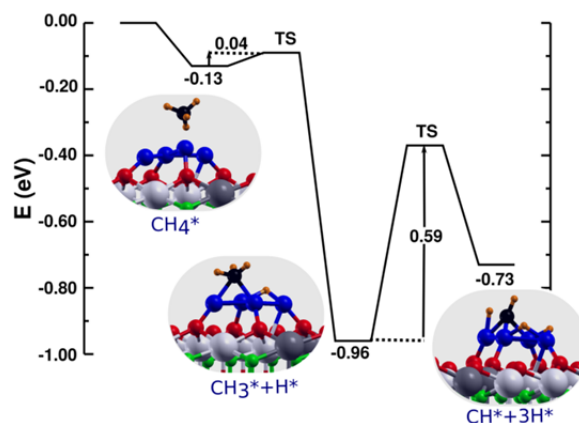
## Results and discussion

Figure 1 displays C 1s XPS spectra acquired after exposing clean Ni(111), CeO<sub>2</sub>(111) and a CeO<sub>2</sub>(111) surface with  $\sim 0.15$  ML of nickel to 1 Torr of methane at 300 K. Ni(111) is frequently used as a benchmark in experimental and theoretical studies for the activation of methane on metal surfaces.<sup>27-29</sup> On the Ni(111) surface, the C 1s XPS spectrum points to a negligible dissociation of methane in agreement with previous studies which show almost no interaction of the molecule with metal surfaces of pure nickel {(100), (110) and (111) terminations} at room temperature.<sup>27-29</sup> On the pristine CeO<sub>2</sub>(111) sample, the adsorption of methane is also negligible. The deposition of small amounts of Ni on a CeO<sub>2</sub>(111) film at 300 K produces a partial reduction of the oxide surface and adsorbed NiO<sub>x</sub> species (Figure S1 in Supporting Information).<sup>16,17</sup> In these systems, individual atoms and tiny clusters (2-10 atoms) of nickel are in close contact with the ceria support.<sup>16-18</sup> The electronic perturbations induced by ceria on the nickel have a strong influence on the reactivity of the system towards methane. The top panel in Figure 1 shows a C 1s XPS spectrum recorded after exposing a CeO<sub>2</sub>(111) surface containing 0.15 ML of nickel to 1 Torr of CH<sub>4</sub> at room temperature for 5 minutes. Over the Ni/CeO<sub>2</sub>(111) surface, methane is activated and decomposes. Clear peaks are seen for CH<sub>x</sub> and CO<sub>x</sub> groups.<sup>18,30</sup> A significant portion of the reacting methane follows a reaction path which leads to full dissociation: CH<sub>4</sub>  $\rightarrow$  CH<sub>3</sub>  $\rightarrow$  CH<sub>2</sub>  $\rightarrow$  CH  $\rightarrow$  C. The calculated reaction profile for the dissociation from CH<sub>4</sub> up to CH is shown in Figure 2 over a flat Ni<sub>4</sub>/CeO<sub>2</sub>(111) model

catalysts where Ni atoms are oxidized ( $\text{Ni}^{0.5+}$ ) and the support is partially reduced (cf. Table S1 and Figure S2),<sup>16</sup> *i.e.*, the computational model matches the essential features of the experimental model catalysts, and there is a clear similarity of the clusters with fragments of Ni(111) terraces. Previous theoretical studies have shown that the binding energy of methane on Ni(111) is negligible ( $<0.1$  eV) with a large activation barrier (0.8–1 eV) for dissociation).<sup>17,31</sup> In contrast, methane reacts with the  $\text{NiO}_x$  species supported on ceria via the formation of a  $\text{CH}_3$  fragment and a H bound to the Ni cluster with a very low activation barrier (0.04 eV). A subsequent dissociation of the methoxy species produces directly CH and 2 Ni–H species with a barrier of 0.59 eV, which is surmounted at experimental conditions. Further dissociation produces C adatoms that react with O atoms from the surface to yield  $\text{CO}_x$  groups.<sup>18</sup> Less than a monolayer of methane reacted with the Ni/CeO<sub>2</sub>(111) system at 300 K and there were no significant changes in the oxidation state of Ni and Ce.



**Figure 1.** C 1s XPS Spectra collected after exposing Ni(111), bottom panel, CeO<sub>2</sub>(111) and Ni/CeO<sub>2</sub>(111), top panel, to 1 Torr of methane at 300 K for 5 minutes. To generate the H<sub>2</sub>O/Ni(111) and H<sub>2</sub>O/Ni/CeO<sub>2</sub>(111) samples, the corresponding surfaces were exposed to 1 Torr of water at 300 K before dosing methane.



**Figure 2.** Energy profile for the  $\text{CH}_4 \rightarrow \text{CH}_3 + \text{H} \rightarrow \text{CH} + 3\text{H}$  reaction on Ni<sub>4</sub>/CeO<sub>2</sub>(111). Energies are referenced to the total energy of CH<sub>4</sub>(g) and the Ni<sub>4</sub>/CeO<sub>2</sub>(111) surface. The structures correspond to the side views of the molecularly adsorbed CH<sub>4</sub> and dissociated states. Atom color key: Ni (blue), Ce<sup>3+</sup> (gray), Ce<sup>4+</sup> (white), surface/subsurface oxygen atoms (red/green), oxygen atoms from chemisorbed species (red), hydrogen (orange), and carbon atoms (black).

Ni(111) interacts poorly with water.<sup>32</sup> After exposing a Ni(111) surface to 1 Torr of water at 300 K, we found a very small amount (< 0.1 ML) of oxygen-containing species on the surface, probably produced by the decomposition of the molecule on defect sites.<sup>32</sup> Pre-dosing with water did not enhance the interaction of methane with Ni(111), bottom panel in Fig 1. On a Ni<sub>4</sub>/CeO<sub>2</sub>(111) substrate, water dissociation,  $\text{H}_2\text{O} \rightarrow \text{OH} + \text{H}$ , is a downhill process (see Figure S3). Experiments of ambient-pressure XPS indicate that H<sub>2</sub>O and OH species are coadsorbed on Ni/CeO<sub>2</sub>(111) surfaces at 300 K when these systems are in equilibrium with a pressure of gaseous water.<sup>33</sup> However, at higher temperatures (> 400 K), only a small amount of OH groups (< 0.3 monolayer) is bonded to the Ni/CeO<sub>2</sub>(111) surfaces.<sup>33</sup> The ability of Ni/CeO<sub>2</sub>(111) to dissociate water<sup>33</sup> can be used to control the reaction selectivity after the activation of CH<sub>4</sub>. When H<sub>2</sub>O is pre-adsorbed on Ni/CeO<sub>2</sub>(111), the selectivity towards the production of CH<sub>x</sub>



groups increases to 100% (top spectrum in Figure 1). OH groups probably block surface sites that are highly active for the complete decomposition of methane, formation of  $\text{Ni(OH)}_2$  is seen in XPS (Figure S1), and the signals for C and  $\text{CO}_x$  groups vanish from the C 1s data. As we will see below, this phenomenon is essential to push the conversion of methane into methanol.

The  $\text{CH}_x$  and OH groups coadsorbed on  $\text{Ni/CeO}_2(111)$  at 300 K do not interact to produce  $\text{CH}_3\text{OH}$ . At this temperature, the system cannot overcome the activation barriers associated with the breaking of HO–surface and  $\text{H}_x\text{C}$ –surface bonds. At a temperature of 450 K, the  $\text{Ni/CeO}_2(111)$  surface is able to catalyze reactions (1) and (2) but a significant production of methanol was seen only in the presence of water. Figure 3 compares the rates for the reactions on  $\text{Ni}(111)$  and  $\text{Ni/CeO}_2(111)$  surfaces as a function of time with a mixture of  $\text{CH}_4$  and  $\text{O}_2$  in the feed.  $\text{Ni}(111)$  displays a very low activity for the combustion of methane to  $\text{CO/CO}_2$  and we did not detect the formation of any methanol on this catalyst. No activity for reactions (1) and (2) was found on plain  $\text{CeO}_2(111)$  under the reaction conditions used for the experiments in Figure 3. In the case of 0.15 ML of Ni on  $\text{CeO}_2(111)$ , we found a very good active and stable catalyst for the combustion of methane with the formation of some methanol. Without water in the reaction feed, the production of methanol is very small and  $\text{CO/CO}_2$  and  $\text{H}_2$  are the main reaction products. The highly active surface sites are not covered by OH species and thus the  $\text{CH}_4 + \text{nO}_2 \rightarrow \text{CO/CO}_2 + \text{H}_2$  reaction occurs instead of  $\text{CH}_3\text{OH}$  formation. Since both reaction pathways are possible from a thermodynamic viewpoint,<sup>2</sup> most of the  $\text{CH}_3\text{OH}$  generated may be decomposed into  $\text{CO/CO}_2$ .<sup>3-6</sup> However, in a water rich environment the catalytic production of methanol increases significantly as shown in Figure 4. At a 4:1 ratio of  $\text{H}_2\text{O}:\text{CH}_4$ , the selectivity towards methanol formation was  $\sim 35\%$ . A higher  $\text{H}_2\text{O}:\text{CH}_4$  ratio did not improve the selectivity for methanol formation and substantially decreased the conversion of methane. OH groups formed

by the dissociation of water on the Ni/CeO<sub>2</sub>(111) surface<sup>33</sup> probably blocked sites necessary for the bonding and activation of methane. The best selectivity towards methanol production observed in this study is larger than the best selectivity reported in the literature for ceria- and zirconia-based powder catalysts which contain NiO as an active phase.<sup>34</sup>

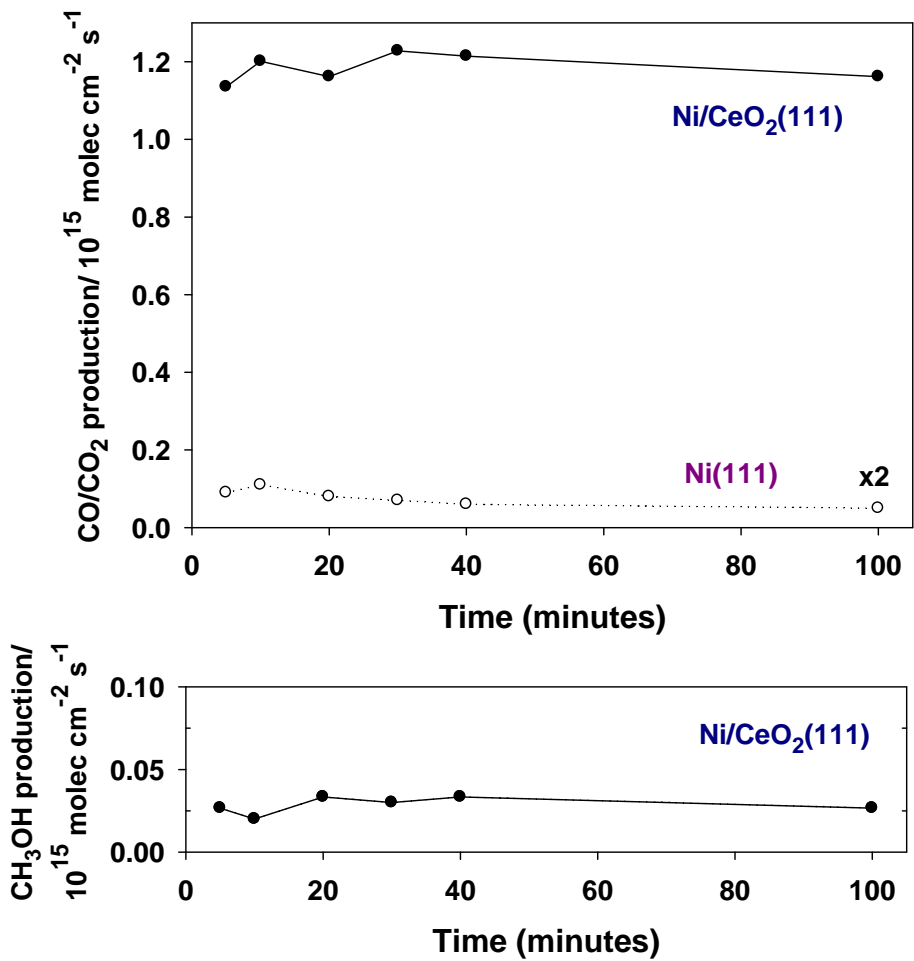


**Figure 3.** Production of CO/CO<sub>2</sub>, top panel, and methanol, bottom panel, on Ni(111) and Ni/CeO<sub>2</sub>(111) catalysts as a function of time. The Ni coverage on ceria was ~ 0.15 ML. The

sample was exposed to 1 Torr of CH<sub>4</sub>, and 0.5 Torr of O<sub>2</sub> at 450 K. No methanol production was detected over the Ni(111) catalyst.

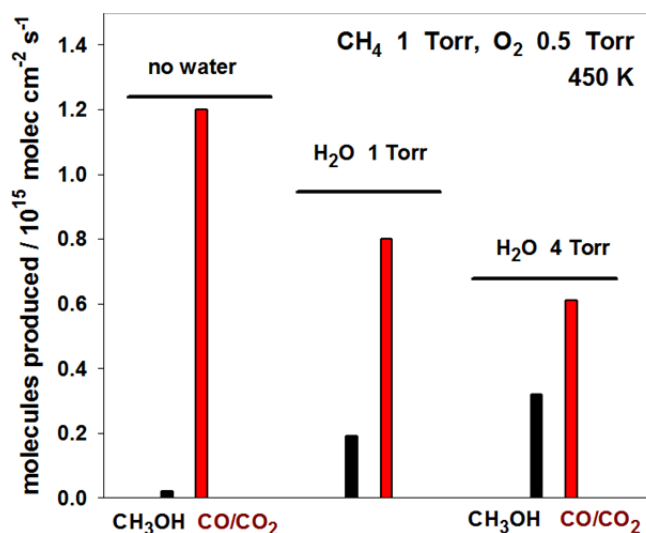


**Figure 4.** Production of methanol on a Ni/CeO<sub>2</sub>(111) catalyst as a function of water pressure. The Ni coverage on ceria was ~0.15 ML. The sample was exposed to 1 Torr of CH<sub>4</sub>, 0.5 Torr of O<sub>2</sub> and 0, 1 or 4 Torr of H<sub>2</sub>O at 450 K.

The results in Figure 3 point to strong effects of metal-support interactions on the catalytic process. Formation of methanol was seen only when a nickel-ceria interface existed and the Ni/CeO<sub>2</sub>(111) catalyst was much more active for the conversion of methane than Ni(111). A plot of the catalytic activity for the production of methanol on Ni/CeO<sub>2</sub>(111) as a function of nickel coverage, Figure 5, also reflects the effects of a strong metal-support interaction. For small coverages of Ni on ceria (< 0.2 ML), results of valence and core-level photoemission show that the oxide induces strong electronic perturbations on nickel.<sup>35</sup> These electronic perturbations decrease at higher Ni coverages and the catalytic activity for the production of CO/CO<sub>2</sub> and CH<sub>3</sub>OH drops. The catalysts with nickel coverages below 0.3 ML did not show any signs for deactivation after performing the reaction for 100 minutes maintaining their activity and selectivity; they did survive several catalytic cycles at a temperature of 450 K.

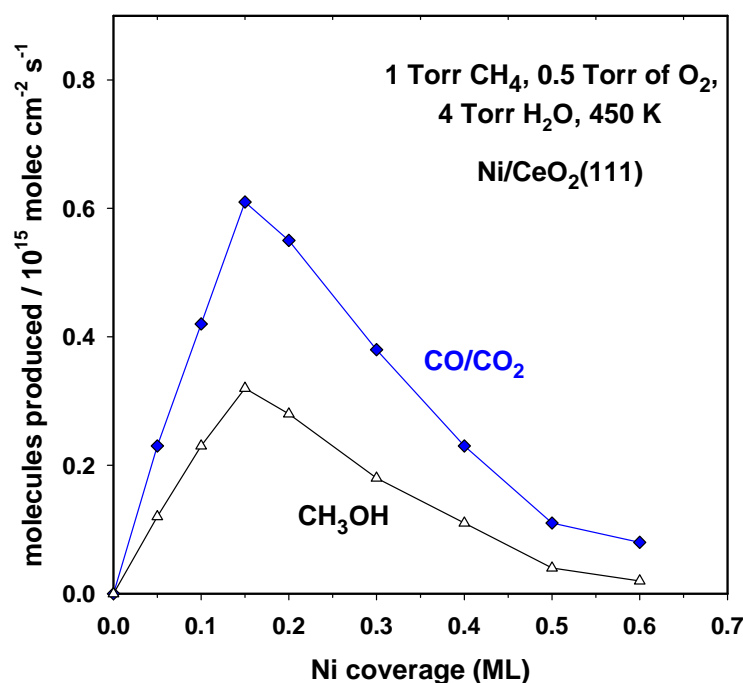


**Figure 5.** Production of CO/CO<sub>2</sub> and CH<sub>3</sub>OH on Ni/CeO<sub>2</sub>(111) catalysts as a function of nickel coverage. The samples were exposed to 1 Torr of CH<sub>4</sub>, 0.5 Torr of O<sub>2</sub> and 4 Torr of H<sub>2</sub>O at 450 K.

Using ambient-pressure X-ray photoelectron spectroscopy (AP-XPS) we investigated the surface chemistry associated with the activation and conversion of methane on Ni/CeO<sub>2</sub>(111). Figure 6 shows C 1s XPS spectra collected while exposing a low-loaded Ni/CeO<sub>2</sub>(111) catalyst to a mixture of CH<sub>4</sub>/O<sub>2</sub> with and without water. As the pressure of water in the background increases, there is an increase in the signal for adsorbed CH<sub>x</sub> groups that can be transformed into methanol with the amount of surface CO<sub>x</sub> present always being small. In the C 1s region we did not see any signal that could be attributed to adsorbed CH<sub>3</sub>O or CH<sub>3</sub>OH. Thus, at 450 K, the CH<sub>3</sub> → CH<sub>3</sub>O → CH<sub>3</sub>OH conversion probably occurs very fast when water is present in the reaction mixture. In principle, the oxygen atom present in methanol could be coming from adsorbed O atoms or OH groups which are present on the surface (Figure S4).

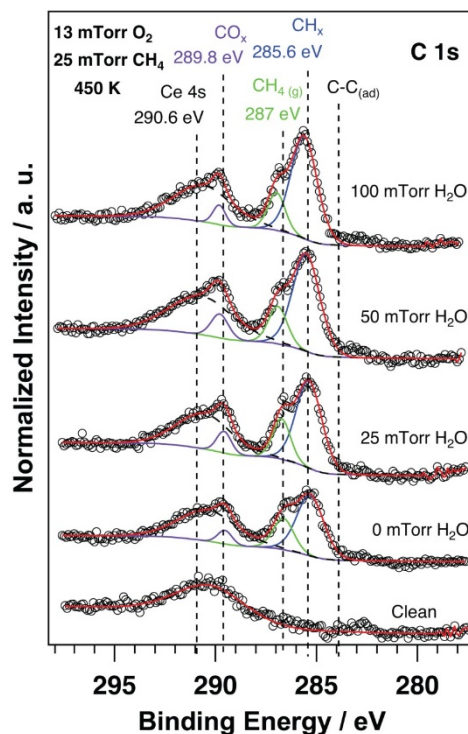


**Figure 6.** C 1s XPS spectra acquired while exposing a CeO<sub>2</sub>(111) surface pre-covered with 0.15 ML of nickel to a reaction mixture of methane (25 mTorr) and O<sub>2</sub> (13 mTorr) without and with water (0, 25, 50, 100 m Torr). The temperature of the sample was 450 K.

Figure 7 displays Ce 4d and Ni 3p XPS spectra collected together with the experiments shown in Figure 6. In Figure 7A, one sees the characteristic line-shape and features for CeO<sub>2</sub>.<sup>17</sup> We found that the hydrogen produced by the dissociation of pure methane at high temperature could reduce the ceria substrate,<sup>34</sup> but in the presence of oxidant agents (O<sub>2</sub>, H<sub>2</sub>O), a reduction process is impossible. This is good because Ce<sup>3+</sup> sites present in ceria could decompose the formed methanol.<sup>36</sup> In Figure 7B, the Ni 3p features exhibit a line-shape that could be a product of the existence of Ni<sup>2+</sup> species, such as Ni(OH)<sub>2</sub> and NiO. The dosing of H<sub>2</sub>O to Ni/CeO<sub>2</sub>(111) at room temperature (Figure S1) produces Ni(OH)<sub>2</sub> as a dominant species, but at 473 K and under a reaction mixture that also contains CH<sub>4</sub> and O<sub>2</sub>, the relative concentration of the nickel hydroxide decreases. A large fraction of the OH groups seen in AP-XPS (Figure S) is probably bound to ceria sites. In the catalysts, Ni could dissociate CH<sub>4</sub>, water and O<sub>2</sub> (which, for our

$\text{Ni}_4/\text{CeO}_2(111)$  theoretical model catalyst, was also considered, see Figs.2, S3 and S5), and ceria probably dissociates  $\text{O}_2$  and water at  $\text{Ce}^{3+}$  sites produced by the Ni deposition. The material was active and stable as a catalyst for the production of methanol only when methane,  $\text{O}_2$  and water were present in the feed. A feed with only methane and  $\text{O}_2$  produced a negligible amount of methanol. For a feed with methane and water, we found a slow reduction of the system and eventual deactivation by carbon deposition. In the absence of  $\text{O}_2$ , the oxidant capacity of water was not able to balance the reducing power of methane.

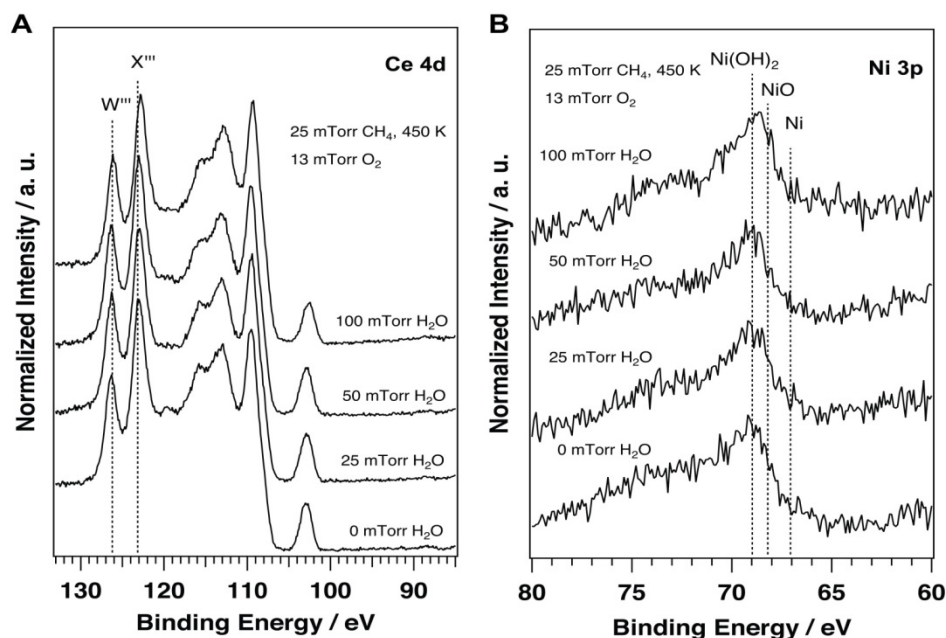


**Figure 7.** Ce 4d and Ni 3p XPS spectra acquired while exposing a  $\text{CeO}_2(111)$  surface pre-covered with 0.15 ML of nickel to a reaction mixture of methane (25 mTorr) and  $\text{O}_2$  (13 mTorr) without and with water (0, 25, 50, 100 m Torr). The temperature of the sample was 450 K.

To obtain microscopic insight into possible reaction paths and the special role of water into the behaviour of the low-loaded  $\text{Ni-CeO}_2(111)$  system for the production of methanol from methane and oxygen, we studied the process by using calculations based on a spin-polarized density functional theory (DFT+U) approach. . We modeled the experimental  $\text{Ni-CeO}_2$  system

using small flat  $\text{Ni}_4$  clusters on a  $\text{CeO}_2(111)$  surface.<sup>16</sup> These  $\text{Ni}_4$  species partially reduce the support, with the formation of two  $\text{Ce}^{3+}$ , *i.e.*, the Ni atoms in direct contact with the reducible ceria support are partially oxidized (cf. Table S1).

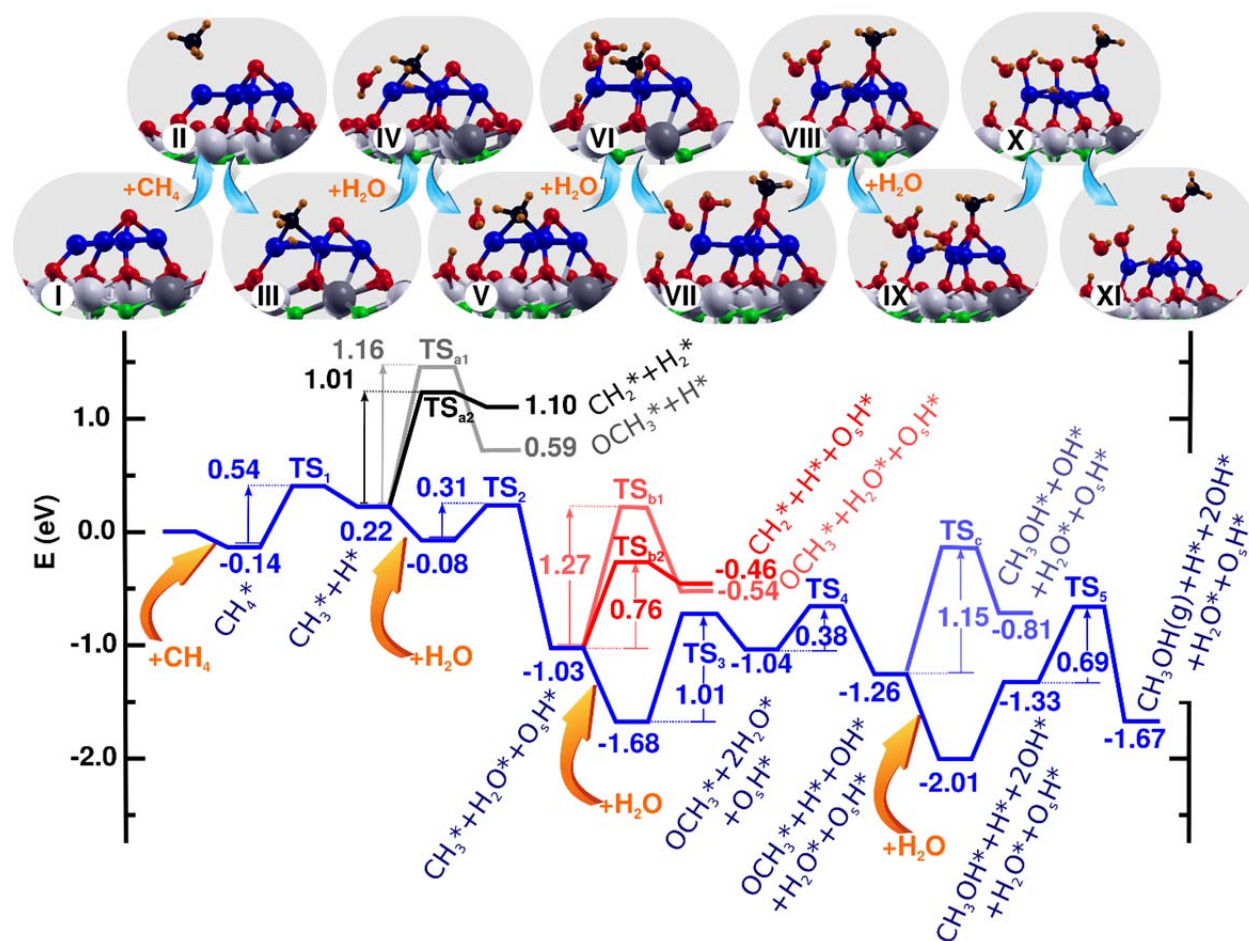


**Figure 8.** Energy profile for the  $\text{CH}_4$  to  $\text{CH}_3\text{OH}$  reaction over an  $\text{O}/\text{Ni}_4/\text{CeO}_2(111)$  surface under the presence of  $\text{H}_2\text{O}$ . Energies are referenced to the total energy of  $\text{CH}_4$  (g),  $3\text{H}_2\text{O}$  (g) and the  $\text{Ni}_4/\text{CeO}_2(111)$  surface with chemisorbed oxygen. The side views of the optimized structures are included. Atom color key: Ni (blue),  $\text{Ce}^{3+}$  (gray),  $\text{Ce}^{4+}$  (white), surface/subsurface lattice oxygen atoms (red/green), oxygen atoms from chemisorbed species (red), hydrogen (orange), and carbon atoms (black). The principal reaction path is depicted in blue, whereas alternative routes are shown in black, gray, red and light red, as well as light blue.

As mentioned above, molecular oxygen readily dissociates to chemisorbed atomic species on the ceria-supported  $\text{Ni}_4$  species (cf. Figure S5). Thus, we considered a partially

oxygen covered  $\text{Ni}_4/\text{CeO}_2(111)$  system to calculate the  $\text{CH}_4$  to  $\text{CH}_3\text{OH}$  reaction profile (Figure 8). The molecular binding of  $\text{CH}_4$  to the oxidized  $\text{Ni}_4$  particles is not that strong (0.14 eV; structure II) with an activation barrier for the first hydrogen abstraction of 0.54 eV ( $\text{TS}_1$ , Figure 8). This is somewhat larger than that for the  $\text{Ni}_4/\text{CeO}_2(111)$  system without chemisorbed oxygen, but is comparable to that for the further decomposition of the methyl species on that system (cf. Figure 2). After the activation of methane on the  $\text{O}/\text{Ni}_4/\text{CeO}_2(111)$  surface, methoxy species could form, but the activation barrier would be large, 1.16 eV ( $\text{TS}_{a1}$ , Figure 8). Instead, the methyl species would dissociate ( $\text{CH}_3 \rightarrow \text{CH}_2 + \text{H}$ ) with a smaller barrier of 1.01 eV ( $\text{TS}_{a2}$ , Figure 8).

The addition of water, however, changes the reaction path.. The adsorbed water molecule (structure IV) dissociates by overcoming a relatively low-energy activation barrier ( $\text{TS}_2 = 0.31$  eV, Figure 8), producing a surface hydroxyl group ( $\text{O}_s\text{H}$ ) on the ceria support (accompanied by the formation of an additional  $\text{Ce}^{3+}$ ), whereas the water OH group recombines with the hydrogen previously abstracted from methane, forming a new adsorbed water molecule (structure V). Once more, methoxy species could form, but the activation barrier would also be large, 1.27 eV ( $\text{TS}_{b1}$ , Figure 8). Instead, the methyl species would dissociate with a smaller barrier of 0.76 eV ( $\text{TS}_{b2}$ , Figure 8). Thus, more water is added to the system (structure VI). At this point, there is enough chemisorbed water to block all Ni sites necessary for methyl species to dissociate relatively easily (cf. Figure S6) and thus a methoxy species forms on nickel (structure VII) via a 1.01 eV transition state ( $\text{TS}_3$ , Figure 8).

Further dissociation of a chemisorbed water species stabilizes the system yielding chemisorbed H and OH species on the nickel cluster (structure VII). The activation energy for the formation of  $\text{CH}_3\text{OH}$  from the chemisorbed  $\text{OCH}_3$  and H species is calculated to be 1.15 eV



(TS<sub>c</sub>, Figure 8), comparable with the methoxy formation barrier. However, if additional water is adsorbed (structure IX), it could donate an H to the methoxy species and thus form CH<sub>3</sub>OH without barrier (structure X). The desorption of methanol occurs via a 0.69 eV transition state (TS<sub>5</sub>, Figure 8) which is accompanied by the adsorption of a OH species at the catalyst site from which CH<sub>3</sub>OH has desorbed.

In the present study, we used ambient pressure X-ray photoelectron spectroscopy and performed DFT+U calculations to elucidate the reaction mechanism for the direct CH<sub>4</sub> conversion to CH<sub>3</sub>OH at the surface of a low-loaded Ni-CeO<sub>2</sub> catalyst. This system exhibits features not seen in catalysts able to perform a CH<sub>4</sub> → CH<sub>3</sub>OH transformation such as copper-exchanged zeolites<sup>6,12</sup> or a model inverse oxide/metal catalyst like CeO<sub>2</sub>/CuO<sub>x</sub>/Cu(111).<sup>14</sup> On one hand, we show that the reducible ceria support modifies the electronic properties of the nickel in direct contact with it, changing its oxidation state while becoming oxidized. This, in turn, results in chemical properties which are very different from those of the corresponding larger three-dimensional nanoparticles or extended nickel surfaces. These metal-support interactions play an essential role in the easy cleavage of O–H and C–H bonds, which is crucial for the dissociation of H<sub>2</sub>O as well as the activation of CH<sub>4</sub> which is needed in the CH<sub>4</sub> conversion to CH<sub>3</sub>OH with O<sub>2</sub> present in the feed. Note that contrary to large three-dimensional Ni nanoparticles, the presence of Ni adatoms, which are oxidized (Ni<sup>2+</sup>), is not detrimental to the activity since O–H and C–H bonds can be easily cleaved over them.<sup>17,33</sup> The metal-support interactions seen in our catalysts lead to a much better selectivity towards methanol production than that observed in other types of ceria- and zirconia-based catalysts.<sup>34</sup> On the other hand, we show that water in excess is absolutely necessary for avoiding the complete decomposition of methane on the partially oxidized Ni nanoparticles, which would yield CO and/or CO<sub>2</sub>. The role

of water is twofold. First, it blocks Ni active sites by dissociating over them, yielding chemisorbed OH and H species. As a consequence, CH<sub>3</sub> would rather form OCH<sub>3</sub> species with existing chemisorbed O species than further decompose. Second, water also helps the formation and desorption of CH<sub>3</sub>OH. Water provides a H atom and a OH species for the Ni–OCH<sub>3</sub>+Ni–H→Ni–OH + Ni + CH<sub>3</sub>OH (g) reaction to occur. On the Ni/CeO<sub>2</sub> surfaces, one sees a reaction mechanism for the direct CH<sub>4</sub> → CH<sub>3</sub>OH conversion not seen over copper-exchanged zeolites<sup>6,12</sup> or model inverse oxide/metal catalyst like CeO<sub>2</sub>/CuO<sub>x</sub>/Cu(111).<sup>14</sup>

## Conclusion

Metal-support interactions and water site-blocking play a crucial role in the conversion of methane to methanol on Ni/CeO<sub>2</sub> catalysts. The metal-support interactions make possible the binding and activation of water and methane at low temperature while the water site-blocking tunes the surface reactivity and enhances the selectivity towards methanol formation. A survey of the literature shows that water also plays an essential role in the step-wise formation of methanol from methane on copper-exchanged zeolites<sup>3,6</sup> and also for the direct catalytic conversion over a model inverse CeO<sub>2</sub>/CuO<sub>x</sub>/Cu(111) catalyst<sup>14</sup> but the interplay between CH<sub>3</sub> species, O adatoms and water molecules is different on a Ni/ceria catalyst. Although water-site blocking is important, one still needs the effects of metal-support interactions to bind and activate methane and water. We believe that the conceptual ideas presented here can be quite useful for the design of other conventional metal/oxide catalysts which can achieve the transformation of methane to methanol.

## Acknowledgements

The work carried out at Brookhaven National Laboratory was supported by the US Department of Energy (Chemical Sciences Division, DE-SC0012704). S.D.S. is supported by a US Department of Energy Early Career Award. This research used resources of the Advanced Light Source (Beamline 9.3.2), which is a DOE Office of Science User Facility under contract no. DE-AC02-05CH11231. Authors acknowledge contribution of Dr. Ethan Crumlin for assistance with AP-XPS measurements. M.V.G.P. acknowledges the financial support of the Ministry of Economy and Competitiveness MINECO-Spain (grant Nr. CTQ2015-78823-R) and P.G.L. that of the Agencia Nacional de Promoción Científica y Tecnológica-Argentina (grant Nr. PICT-2016-2750). Computer time provided by the BIFI-ZCAM, RES at the Marenostrum and LaPalma nodes, SNCAD (Sistema Nacional de Computación de Alto Desempeño, Argentina), and the DECI resources BEM based in Poland at WCSS and Archer at EPCC with support from the PRACE aislb, is acknowledged. M.V. thanks the Ministry of Education, Youth and Sports of the Czech Republic for financial support under project LH15277.

## Additional information

**Supplementary Information** accompanies this paper at xxx, and it includes XPS spectra, structural  $\text{Ni}_4/\text{CeO}_2(111)$  model and Bader charges as well as reaction profiles calculated with DFT. Geometries of all the stationary points and transition state structures whose relative energies are given in the manuscript, along with their calculated absolute energies and number of imaginary frequencies.

**Competing financial interests:** The authors declare no competing financial interests.

## References

1. *Methane in the Environment: Occurrence, Uses and Pollution*, A. Basile (Editor), Nova Science Publication Inc, 2013.
2. Khirsariya, P.; Mewada, R.K. Single step oxidation of methane to methanol – towards better understanding. *Procedia Engineering* **51**, 409–415 (2013).
3. Grundner, S.; Markovits, M.A.C.; Li, G.; Tromp, M.; Pidko, E.A.; Hensen, E.J.M.; Jentys, A.; Sanchez-Sanchez, M.; Lercher, J. A. Single-site trinuclear copper oxygen clusters in mordenite for selective conversion of methane to methanol. *Nature Communications* **6**, 7546–7555 (2013).
4. Li, G.; Vassilev, P.; Sanchez-Sanchez, M.; Lercher, J.A.; Hensen, E.J.M.; Pidko, E.A. Stability and reactivity of copper oxo-clusters in ZSM-5 zeolite for selective methane oxidation to methanol. *J. Catal.* **338**, 305–312 (2016).
5. Tomkins, P.; Ranocchiari, M.; van Bokhoven, J.A. Direct conversion of methane to methanol under mild conditions over Cu-zeolites and beyond. *Acc. Chem. Res.* **50**, 418–425 (2017).
6. Sushkevich, V.L.; Palagin D.; Ranocchiari, M.; van Bokhoven, J.A. Selective anaerobic oxidation of methane enable direct synthesis of methanol. *Science* **356**, 523–527 (2017).
7. Chan, S.I.; Yu, S.S.-F. Controlled oxidation of hydrocarbons by the membrane-bound methane monooxygenase: The case for a tricopper cluster. *Acc. Chem. Res.* **41**, 969–979 (2008).
8. Chan, S.I.; Lu, Y.-J.; Nagababu, P.; Maji, S.; Hung, M.C.; Lee, M.M.; Hsu, I.-J.; Minh, P.D.; Lai, J.C.-H.; Ng, K.Y.; Ramalingam, S.; Yu, S.S.-F.; Chan, M.K. Efficient oxidation of methane to methanol by dioxygen mediated by tricopper clusters. *Angew. Chem. Int. Ed.* **52**, 3731–3735 (2013).
9. Xu, J.; Zheng, A.; Wang, X.; Qi, G.; Su, J.; Du, J.; Gan, Z.; Wu, J.; Wang, W.; Deng, F. Room temperature activation of methane over Zn modified H-ZSM-5 zeolites: Insight from solid-state NMR and theoretical calculations. *Chem. Sci.* **3**, 2932–2940 (2012).
10. Olivos-Suarez, A.I.; Szécsényi, A.; Hensen, E.J.M.; Ruiz-Martinez, J.; Pidko, E.A.; Gascon, J. Strategies for the direct catalytic valorization of methane using heterogeneous catalysis: Challenges and opportunities. *ACS Catal.* **6**, 2965–2981 (2016).
11. Chin, Y.-H.; Buda, C.; Neurock, M.; Iglesia, E. Consequences of metal–oxide interconversion for C–H bond activation during CH<sub>4</sub> reactions on Pd catalysts. *J. Am. Chem. Soc.* **135**, 15425–15442 (2013).
12. Narsimhan, K.; Iyoki, K.; Dinh, K.; Román-Leshkov, Y. Catalytic oxidation of methane into methanol over copper-exchanged zeolites with oxygen at low temperature. *ACS Cent. Sci.* **2**, 424–429 (2016).
13. Ravi, M.; Ranocchiari, M.; van Bokhoven, J.A. The Direct Catalytic Oxidation of Methane to Methanol—A Critical Assessment. *Angew. Chem. Int. Ed.* **56**, 16464–16483 (2017).
14. Zuo Z.; Ramirez, P. J.; Sennayake, S. D.; Liu, P.; Rodriguez, J. A. Low-Temperature Conversion of Methane to Methanol on CeO<sub>x</sub>/Cu<sub>2</sub>O Catalysts: Water Controlled Activation of the C–H Bond. *J. Am. Chem. Soc.* **138**, 13810–13813 (2016).
15. Pappas, D.K.; Borfecchia, E.; Dyballa, M.; Pankin, I.A.; Lomachenko, K.A.; Martini, A.; Signorile, M.; Teketel, S.; Arstad, B.; Berlier, G.; Lamberti, C.; Bordiga, S.; Olsbye, U.; Lillerud, K.P.; Svelle, S.; Beato P. Methane to Methanol: Structure–Activity Relationships for Cu-CHA. *J. Am. Chem. Soc.* **139**, 14961–14975 (2017).

16. Carrasco, J.; Barrio, L.; Liu, P.; Rodriguez, J.A.; Ganduglia-Pirovano, M.V. Theoretical studies of the adsorption of CO and C on Ni(111) and Ni/CeO<sub>2</sub>(111): Evidence of a strong metal–support interaction. *J. Phys. Chem. C* **117**, 8241–8250 (2013).
17. Lustemberg, P.G.; Ramírez, P.J.; Liu, Z.; Ramón A. Gutiérrez, R.A.; Grinter, D.G.; Carrasco, J.; Senanayake, S.D.; Rodriguez, J.A.; Ganduglia-Pirovano, M.V. Room-temperature activation of methane and dry re-forming with CO<sub>2</sub> on Ni–CeO<sub>2</sub>(111) surfaces: Effect of Ce<sup>3+</sup> sites and metal–support interactions on C–H bond cleavage. *ACS Catal.* **6**, 8184–8191 (2016).
18. Liu, Z.; Grinter, D.G.; Lustemberg, P.G.; Nguyen-Phan, T.-D.; Zhou, Y.; Luo, S.; Waluyo, I.; Crumlin, E.J.; Stacchiola, D.J.; Zhou, J.; Carrasco, J.; Busnengo, H.F.; Ganduglia-Pirovano, M.V.; Senanayake, S.D.; Rodriguez, J.A.. Dry reforming of methane on a highly-active Ni–CeO<sub>2</sub> catalyst: Effects of metal-support interactions on C–H bond breaking. *Angew. Chem. Int. Ed.* **55**, 7455–7459 (2016).
19. Dudarev, S.; Botton, G.; Savrasov, S.; Humphreys, C.; Sutton, A. Electron-energy-loss spectra and the structural stability of nickel oxide: An LSDA+U study. *Phys. Rev. B* **57**, 1505–1509 (1998).
20. Perdew, J. P.; Burke, K.; Ernzerhof, M. Generalized gradient approximation made simple. *Phys. Rev. Lett.* **77**, 3865–3868 (1996).
21. <http://www.vasp.at>; version vasp.5.3.5.
22. Fabris, S.; Vicario, G.; Balducci, G.; de Gironcoli, S.; Baroni, S. Electronic and atomistic structures of clean and reduced ceria surfaces. *J. Phys. Chem. B* **109**, 22860–22867 (2005).
23. Cococcioni, M.; de Gironcoli, S. Linear response approach to the calculation of the effective Interaction parameters in the LDA+U method. *Phys. Rev. B* **71**, 35105–35120 (2005).
24. Kresse, G.; Joubert, D. From ultrasoft pseudopotentials to the projector augmented-wave method. *Phys. Rev. B* **59**, 1758–1775 (1999).
25. Blöchl, P. E. Projector augmented-wave method. *Phys. Rev. B* **50**, 17953–17979 (1994).
26. Henkelman, G.; Uberuaga, B.P.; Jónsson, H. A climbing image nudged elastic band method for finding saddle points and minimum energy paths. *J. Chem. Phys.* **113**, 9901–9904 (2000).
27. Beebe Jr., T. P.; Goodman, D. W.; Kay, B. D. Kinetics of the activated dissociative adsorption of methane on the low index planes of nickel single crystal surfaces. *J. Chem. Phys.* **87**, 2305–2315 (1987).
28. Campbell, R. A.; Szanyi, J.; Lenz, P. Methane activation on clean and oxidized Ni(100). *Catal. Lett.* **17**, 39–46 (1993).
29. Yuan, K.; Zhong, J.-Q.; Zhou, X.; Xu, L.; Bergman, S.L.; Wu, K.; Xu, G.Q.; Bernasek, S.L.; Li, H.X.; Chen, W. Dynamic Oxygen on Surface: Catalytic Intermediate and Coking Barrier in the Modeled CO<sub>2</sub> Reforming of CH<sub>4</sub> on Ni (111). *ACS Catal.* **6** (7), 4330–4339 (2016).
30. Liu, Z.; Duchoň, T.; Wang, H.; Peterson, E.W.; Zhou, Y.; Luo, S.; Zhou, J.; Matolín, V.; Stacchiola, D.J.; Rodriguez, J.A.; Senanayake, S.D. Mechanistic insights of ethanol steam reforming over Ni–CeO<sub>x</sub>(111): The importance of hydroxyl groups for suppressing coke formation. *J. Phys. Chem. C* **119**, 18248–18256 (2015).
31. Zhou, X.; Nattino, F.; Zhang, Y.; Chen, J.; Kroes, G.-J.; Guo, H.; Jiang, B. Dissociative chemisorption of methane on Ni(111) using a chemically accurate fifteen dimensional potential energy surface. *Phys. Chem. Chem. Phys.*, **19**, 30540–30550 (2017).
32. Zhao, W.; Carey, S.J.; Mao, Z.; Campbell, C.T. Adsorbed Hydroxyl and Water on Ni(111): Heats of Formation by Calorimetry. *ACS Catal.* **8**, 1485–1489 (2018).
33. Carrasco, J.; López-Durán, D.; Liu, Z.; Duchoň, T.; Evans, J.; Senanayake, S.D.; Crumlin, E.J.; Matolín, V.; Rodriguez, J.A.; Ganduglia-Pirovano, M.V. In situ and theoretical studies for the dissociation of water on an active

Ni/CeO<sub>2</sub> catalyst: Importance of strong metal–support interactions for the cleavage of O–H bonds. *Angew. Chem. Int. Ed.* **54**, 3917–3921 (2015).

34. Okolie, C.; Belhseine, Y.F.; Lyu, Y.; Yung, M.M.; Engelhard, M.H.; Kovarik, L.; Stavitski, E.; Sievers, C. Conversion of methane into methanol and ethanol over nickel oxide on ceria-zirconia catalysts in a single reactor. *Angew. Chem. Int. Ed.* **56**, 13876–13881 (2017).

35. Senanayake, S.; Evans, J.; Agnoli, S.; Barrio, L.; Chen, T.-L.; Hrbek, J.; Rodriguez, J. A. Water–Gas Shift and CO Methanation Reactions over Ni–CeO<sub>2</sub>(111) Catalysts. *Topics in Catal.* **54**, 34–41 (2011).

36. Albrecht, P.M.; Mullins, D.R. Adsorption and reaction of methanol over CeO<sub>x</sub>(100) thin films. *Langmuir* **29**, 4559–4567 (2013).

## TOC

